JOURNAL OF THE ROYAL SOCIETY Interface

# The management of fluid and wave resistances by whirligig beetles

Jonathan Voise and Jérôme Casas

*J. R. Soc. Interface* 2010 **7**, 343-352 first published online 29 July 2009
doi: 10.1098/rsif.2009.0210

JOURNAL OF THE ROYAL SOCIETY Interface

*J. R. Soc. Interface* (2010) **7**, 343–352
doi:10.1098/rsif.2009.0210
*Published online* 29 July 2009

# The management of fluid and wave resistances by whirligig beetles

**Jonathan Voise* and Jérôme Casas**

*Université de Tours, IRBI UMR CNRS 6035, Parc Grandmont, 37200 Tours, France*

Whirligig beetles (Coleoptera: Gyrinidae) are semi-aquatic insects with a morphology and propulsion system highly adapted to their life at the air–water interface. When swimming on the water surface, beetles are subject to both fluid resistance and wave resistance.

The purpose of this study was to analyse swimming speed, leg kinematics and the capillarity waves produced by whirligig beetles on the water surface in a simple environment. Whirligig beetles of the species *Gyrinus substriatus* were filmed in a large container, with a high-speed camera. Resistance forces were also estimated.

These beetles used three types of leg kinematics, differing in the sequence of leg strokes: two for swimming at low speed and one for swimming at high speed. Four main speed patterns were produced by different combinations of these types of leg kinematics, and the minimum speed for the production of surface waves (23 cm $s^{-1}$) corresponded to an upper limit when beetles used low-speed leg kinematics. Each type of leg kinematics produced characteristic capillarity waves, even if the beetles moved at a speed below 23 cm $s^{-1}$. Our results indicate that whirligig beetles use low- and high-speed leg kinematics to avoid maximum drag and swim at speed corresponding to low resistances.

**Keywords: air–water interface; capillarity waves; Gyrinidae *Gyrinus substriatus*; leg kinematics; locomotion; movement**

## 1. INTRODUCTION

The air–water interface is an unusual environment, and surface tension and capillarity phenomena are very important for the small animals inhabiting this environment, such as insects, spiders and gastropods (Bush & Hu 2006; Lee *et al.* 2008). Many of the arthropods living in this environment walk on the water surface and have specially adapted integuments, allowing them to be supported by the surface tension (Bush *et al.* 2008). Whirligig beetles (Coleoptera: Gyrinidae) are among the insects living on the water surface and are unusual in that they have their bodies partly immersed in the water (figure 1*a*). This feature poses specific problems and has resulted in the evolution of specific morphological adaptations. As in most aquatic beetles, the body shape of these beetles minimizes resistance when they are swimming (Nachtigall 1974, 1981). Whirligig beetles also display a more specific modification of the eye, making it possible to see both in the air above and in the water below. Each of their compound eyes is divided into two parts, one below and the other above the water line (Hatch 1927). The middle and hind legs of whirligig beetles have also evolved into swimming blades used for propulsion (figure 1*b*). Nachtigall (1961, 1974), who described in detail the rowing kinematics of these legs, indicated that during the power phase (i.e. backward movement), the legs are spread out under pressure and have a contact area 40 times greater than that during the recovery phase (i.e. forward movement). He found that 84 per cent of the energy that *Gyrinus substriatus* Steph. devotes to swimming is transformed into thrust. This efficiency is the highest ever measured for a thrust apparatus in the animal kingdom on the basis of resistance principles (Nachtigall 1961). The hind legs of *G. substriatus* can move at a rate of 60 strokes $s^{-1}$, whereas the middle legs move at half this frequency (Nachtigall 1961). When the beetle is swimming in a straight line, the left and right legs act simultaneously but, during turning manoeuvres, the legs paddle in an asymmetric manner (Fish & Nicastro 2003).

The partial immersion of their bodies in the water results in whirligig beetles being subject to two resistance forces when moving on the water surface. The first force is the fluid resistance, resulting from the energy transmitted to the water by pressure drag, friction and the formation of vortices (Ziegler 1998). The second force is the wave resistance, which is associated with the energy transmitted to the surface waves (Lighthill 1978). These resistance forces can limit the displacement of aquatic or semi-aquatic arthropods, but many of these insects also use fluid or wave resistance to drive propulsion (Nachtigall 1974; Suter *et al.* 1997; Hu *et al.* 2003; Buhler 2007). The relative importance of the two resistance forces is unknown for situations in which these forces oppose the movement of the insect. However, Buhler (2007) indicated that, for water striders (Hemiptera: Gerridae), when both forces contribute to propulsion, fluid and wave drag create two-thirds and one-third of the horizontal momentum transfer, respectively.

*Author for correspondence (jonathan.voise@etu.univ-tours.fr).

*Received* 2 June 2009
*Accepted* 6 July 2009

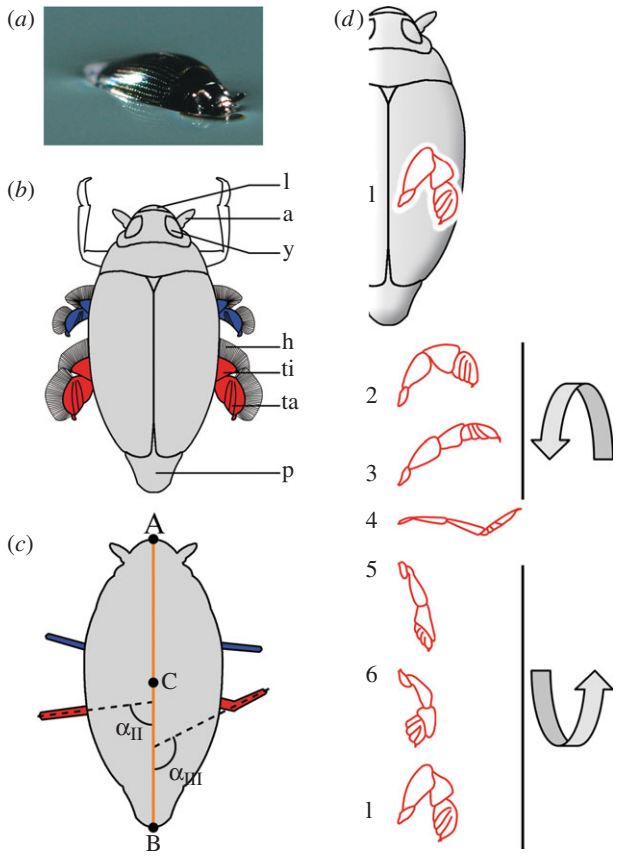


Figure 1. (*a*) Close-up picture of a whirligig beetle (*Gyrinus substriautus*) at rest on the water surface. (*b*) Schematic drawing of a whirligig beetle in dorsal view. Middle legs are represented in blue, and hind legs in red. Forelegs that remain folded under the body during swimming are shown in white. a, Antennae; h, hairs of the swimming blades; l, labium; p, pygidium; ta, tarsi; ti, tibia; y, eye. (*c*) Whirligig beetle with (A) the end of the labium, (B) the end of the pygidium and (C) the centre of the body. The orange line represents the body axis. Middle legs are represented in blue, and hind legs in red. The angles $\alpha_{II}$ and $\alpha_{III}$ represent the maximum angles of the hind legs measured for leg kinematics types II and III, respectively (see the text for more detailed explanation). (*d*) Kinematics of the right hind leg (in red) during a stroke, seen from above (modified from Nachtigall 1961). Each position of the leg is separated by 2 ms. In (4), the position of tarsi is that produced by type III leg kinematics; for type II leg kinematics, the tibia and tarsi stay in the same axis. Three-dimensional arrows indicate the rotation of the leg during the stroke.

Whirligig beetles are very sensitive to the propagation of waves on the water surface and can detect waves with an amplitude of a few micrometers with their antennae (Rudolph 1967). The antenna is formed by a floating haired pedicellus moving with the surface waves, topped by a flagellum amplifying the movement. This, in turn, excites the organ of Johnston within the pedicellus (Eggers 1926, 1927; Wilde 1941). Whirligig beetles seem to use surface waves for detecting predators and prey (Rudolph 1967; Kolmes 1983), chasing behaviour (Bendele 1986) and precopulatory behaviour (Kolmes 1985). They produce surface waves of both the capillarity and gravity-induced types, with a circular or V shape (Tucker 1969). It has been suggested that whirligig beetles may use the echo of their own waves to detect objects on the surface or to avoid obstacles, such as the walls of an aquarium (Eggers 1927; Wilde 1941; Tucker 1969). The presence of an active echolocation system in these insects remains unproven, but it is clear that surface waves play an important role in the orientation of these insects.

Whirligig beetles were so named due to the characteristic circling trajectories they trace on the surface of the water. The geometry of beetle trajectories on the water surface has been studied on several occasions (e.g. Reinig & Uhlemann 1973; Bendele 1986; Winkelman & Vinyard 1991), but surprisingly little is known about the speed at which these beetles move. Speed is an important parameter determining the amplitude of the resistance forces and the shape of surface waves produced (Tucker 1969). Most of the reported data for speed have concerned only maximum speed, which varies from 53 to 144 cm $s^{-1}$ (Tucker 1969; Vulinec 1987). The only comprehensive speed patterns reported to date relate to chasing behaviour and were provided by Bendele (1986). They show the beetle's speed to be irregular, with strong acceleration and deceleration.

The aim of this study was to analyse the swimming speed of whirligig beetles on the water surface in a simple environment. We analysed leg kinematics, quantified speed dynamics for relatively long periods, and characterized the different kinds of capillarity waves produced. We also quantified fluid and wave resistances. We are ultimately interested in the relationship between speed patterns and wave production. A classification based on leg kinematics helped to order the vast array of patterns observed.

## 2. MATERIAL AND METHODS

### 2.1. Beetles

Whirligig beetles of the species *G. substriatus* were collected from a small river and a pond in Indre-et-Loire, France. They were kept in 10 l aquariums, in groups of 8–10, and were fed daily with *Drosophila*. Aquariums were filled with tap water, which was changed weekly.

### 2.2. Video recording

For studies of leg kinematics and speed, beetles were placed individually in a white plastic tank 0.9 m in diameter and 0.6 m high, filled with tap water. A water depth of 10 cm is sufficient for deep water condition for capillarity waves (Dean & Dalrymple 1991).

Whirligig beetles were filmed with a Fastec Imaging TroubleShooter high-speed camera equipped with a Computar zoom lens (18-108/2.5). Video resolution was 640 × 480 pixels. Light was provided by four 500 W projectors. The camera and lights were fixed on a 1 × 1 × 2 m aluminum structure placed above the tank. The lights were at a height of 1 m and the camera was at a height of 1.2 m or 2 m.

Two kinds of video sequence were recorded. The first type of sequence was used to analyse leg kinematics.

The camera was positioned 1.2 m above the plastic tank and the focal length of the zoom lens was set to the minimum value to obtain the best possible resolution of the beetle's legs. All four projectors were switched on. Video sequences were recorded at a speed of 1000 frames $s^{-1}$ for the precise analysis of leg strokes.

The purpose of the second kind of video sequence was to record trajectories and the speed of whole beetles in a simple environment. A large visual field was necessary, so the camera was fixed at a height of 2 m, on top of the aluminum structure. Videos were recorded at a rate of 50 frames $s^{-1}$ and the focal length of the zoom lens was set at its maximum value. Only two projectors on opposite sides of the tank were switched on.

The camera was focused on a dead beetle, and a floating ruler was used for scale. The water was maintained at ambient temperature (approx. 20°C). We avoided leaving the lights on for too long, to prevent large increases in the temperature of the water in the tank. The water was kept as clean as possible and floating dust was regularly removed. For some recordings, a visual stimulus (the experimentator's hand) was applied at the start.

### 2.3. Analysis of leg kinematics

More than 80 video sequences of 12 beetles were recorded for the analysis of leg kinematics. This analysis focused on the succession of strokes carried out by the middle and hind legs. Forelegs (figure 1*b*) were not considered in our study as they are used only for capturing prey, walking or holding on to the substrate, and are folded under the body during swimming. Leg movements were easily discernable on video sequences despite the presence of waves produced by the insect, as major surface deformations occurred mostly in front of or behind the beetle's body, whereas the legs moved at the side of the body. The spatial resolution of the legs (8–9 pixels for hind legs and 5–6 pixels for middle legs) was sufficient for precise determination of the time point at which they started moving backward and to measure the angle they formed with the body.

The *stroke pattern*—the simplest succession of middle and hind leg strokes repeating itself over time—was used to differentiate different *types of leg kinematics*. For each type, we analysed 10 video sequences from five individuals (two videos per beetle). When more than two video sequences were recorded for each type of leg kinematics for a given individual, we selected the two sequences for which a maximum number of stroke patterns could be analysed.

Recorded sequences were analysed frame by frame. For each frame, the positions of the labium end and pygidium end were recorded with ImageJ (http://rsb.info.nih.gov/ij/). These two points were used to calculate the coordinates of the centre of the body and to measure the speed of the beetle (figure 1*c*). Whole body speed was measured with subsampling at 250 frames $s^{-1}$ from the sequences recorded at 1000 frames $s^{-1}$, providing a sufficiently high level of accuracy and avoiding many of the irregularities observed at higher frame rates. We also determined when the middle and hind leg strokes began. A stroke was considered to have started when the unfolded leg started to move backwards and propulsion began (figure 1*d*, beginning of the stroke between positions 3 and 4).

Beetle speed was not constant and the insects moved forwards through a succession of propulsion episodes. A *propulsion episode*, as defined by Suter *et al.* (1997), consists of an increase in speed (acceleration phase) due to a stroke, followed by a decrease in speed due to resistance forces (deceleration phase). The minimum and maximum speeds of the propulsion episodes were determined graphically (figure 2). We calculated the time between two minima and converted it into a frequency, corresponding to the frequency of propulsion episodes. The time and speed between maxima and minima were used to determine acceleration. When a middle leg stroke followed a hind leg stroke during a propulsion episode, we calculated the time between the start of the two strokes.

We also measured the maximum angle between the legs and the body axis of the beetle during a stroke (figure 1*c*). In some cases, legs were bent during strokes, under the action of the resistance forces (figure 1*d*, position 4). As this deformation mostly affected the tarsi, the maximum angle of the tarsi was considered to be the maximum angle of the leg (figure 1*c*). The maximum angle of a stroke was calculated as the mean of the maximum angles of the left and right legs. All the analyses were carried out and the graphs plotted with MatLab 7.0.4.

### 2.4. Statistical analysis

The number of propulsion episodes analysed differed between video sequences. We therefore calculated the mean of each parameter for each video and the means for each type of leg kinematics from the means of the 10 video sequences. This process ensured that all video sequences and all individuals were given equal weighting. The means of the measured parameters were compared by one-way analysis of variance (ANOVA) and Tukey multiple comparison tests, using Tukey's honestly significant difference criterion.

### 2.5. Speed and trajectory analysis

Forty-four video sequences filmed at a rate of 50 frames $s^{-1}$ were used for the analysis of whole-beetle speed. These sequences were obtained with 16 beetles, and 20 s of each video was analysed. The sequences for analysis were selected on the basis of their having the largest possible ranges of speed patterns. Trajectories were reconstructed from the displacement of the centre of the body.

### 2.6. Surface waves

Surface waves produced by strokes and whole-body movement were observed on the video sequences. We also photographed swimming beetles to illustrate the characteristic waves induced by each type of stroke pattern.

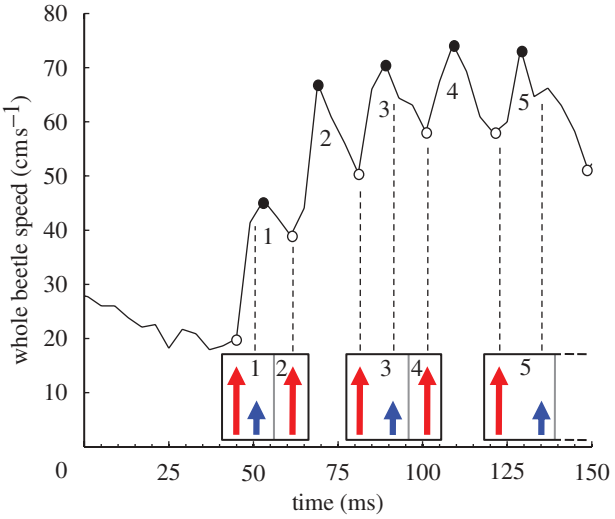


Figure 2. Example of the whole-body speed of *G. substriatus* measured over time for type III leg kinematics. Small blue arrows represent the beginning of middle leg strokes and larger red arrows represent the beginning of hind leg strokes. Each numbered speed peak corresponds to a propulsion episode, with minima indicated by white circles and maxima by black circles. Rectangles identify the stroke patterns. Within a pattern, the stroke or strokes responsible for single propulsion episodes are separated by grey lines, with the number of the propulsion episode generated indicated. $\mathrm{Min}_1$ and $\mathrm{Min}_2$ correspond to the beginning of propulsion episode 1 and propulsion episode 2, respectively. $\mathrm{Max}_1$ indicates the maximum speed reached during propulsion episode 1. The difference in speed between $\mathrm{Max}_1$ and $\mathrm{Min}_1$ gives the gain of speed.

### 2.7. Resistance forces

We studied changes in fluid resistance and wave resistance with beetle velocity. The fluid resistance ($R_f$) corresponds to the force transmitted to the medium (water). This force is given by

$$R_f = \frac{c_w F \rho V^2}{2}, \tag{2.1}$$

where $c_w$ is the coefficient of resistance, $F$ the frontal area of the body in contact with the water, $\rho$ the density of the medium and $V$ the speed of the beetle (Ziegler 1998). Fluid resistance was calculated as the ratio between the value at a given speed and the value obtained at 80 cm s$^{-1}$, which was the maximum speed measured for *G. substriatus* in our experiments. This non-dimensionalization process resulted in a relationship between fluid resistance and speed that was insensitive to the exact value of $c_w$ and $F$, assuming that these two parameters did not depend on beetle speed. It was therefore unnecessary to measure these parameters for determination of the shape of the curve of fluid resistance as a function of beetle speed.

The wave resistance ($R_w$), corresponding to the energy transmitted to the surface waves, was calculated for an object simulated as an external source of pressure moving in a straight line at uniform speed (Chepelianskii *et al.* 2008). Wave drag is then given by

$$R_w = \int_0^\infty dk \frac{k}{2\pi\rho} \frac{P_{\mathrm{ext}}^2(k)\theta(V - c(k))}{V^2\sqrt{1 - (c(k)/V)^2}}, \tag{2.2}$$

where $k$ is the wavenumber, $P_{\mathrm{ext}}(k)$ the pressure source, $c(k)$ the wave velocity and $\theta$ a Heaviside step function (see Chepelianskii *et al.* 2008 for more details). The pressure source was calculated as $P_{\mathrm{ext}}(k) = p_0 \exp(-kb)$, with $p_0$ the total force exerted on the water surface, and $b$ the size of the object. We calculated $R_w$ for an object of 6 mm, the mean size of *G. substriatus*. The value obtained for wave resistance was non-dimensioned by its maximum value.

## 3. RESULTS

### 3.1. Types of leg kinematics

Whirligig beetles used three different types of leg kinematics. These types—types I, II and III—differed in terms of the stroke pattern used (figure 3). Type I was the simplest, and consisted of one middle leg stroke only. The type II stroke pattern was characterized by a rapid succession of one hind leg stroke and one middle leg stroke. The type III stroke pattern was a succession of three strokes, with two hind leg strokes separated by one middle leg stroke.

For types I and II, a single stroke pattern induced a single propulsion episode. For type III, a single stroke pattern generated two propulsion episodes. These episodes were induced by the succession of one hind leg stroke and one middle leg stroke, and by a single hind leg stroke only (figure 2). In the first case, the middle leg stroke occurred during the acceleration phase (figure 2, propulsion episode 1) or during the deceleration phase. If the middle leg stroke occurred during the deceleration phase, it resulted in no increase in speed (figure 2, propulsion episode 3) or a very small acceleration (figure 2, propulsion episode 5).

For propulsion episodes resulting from a hind leg stroke and a middle leg stroke, the time between the beginning of the two strokes (table 1) did not differ significantly between types II and III (ANOVA, $p > 0.05$).

The maximum angle of the hind legs differed significantly between types II and III (ANOVA, $p < 0.001$). The three different types also presented significant differences in the maximum angle of the middle legs (Tukey, $p < 0.05$). Typical maximum angles of the hind legs for types II and III are shown in figure 1*c*. The tibia and tarsi of the hind legs lay along the same axis for type II, whereas the angle of the tarsi was greater than the angle of the tibia for type III. The tibia and tarsi of the middle legs lay along the same axis for type III and the angle of the tarsi was greater than that of the tibia for the other two types (figure 1*c*,*d*). The ratio between the maximum angles of the hind legs and middle legs was 0.80 for type II and 1.35 for type III.

The frequency of propulsion episodes, acceleration and whole-beetle speed for each type of leg kinematics are listed in table 1. These parameters were similar for

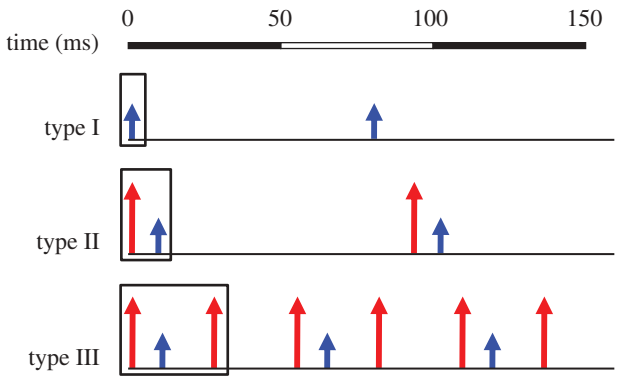


Figure 3. Stroke patterns of the three types of leg kinematics observed for *G. substriatus* swimming on the water surface. Small blue arrows represent the beginning of middle leg strokes and larger red arrows represent the beginning of hind leg strokes. Rectangles identify the stroke pattern of each type of leg kinematics. The time intervals between each stroke are reported in table 1.

types I and II (Tukey, $p > 0.05$), but were significantly different for type III (Tukey, $p < 0.001$).

Figure 4 shows the gain of speed in an acceleration phase plotted against the speed before the acceleration phase for all the propulsion episodes analysed. For type III, no difference in gain of speed was observed between propulsion episodes produced by a single hind leg stroke or by the succession of a hind leg stroke and a middle leg stroke, so these two types of propulsion episode were grouped together. For the same starting speed before the acceleration phase, a greater increase in speed was observed for type II than for type I, and for type III than for types I and II. For all three types of leg kinematics, the gain of speed decreased with increasing speed at the beginning of the propulsion episode.

### 3.2. Beetle speed and trajectories

Large-scale video sequences of the speed of the beetle (i.e. at the scale of the water tank) showed four main patterns of speed (figure 5). The first corresponded to beetles swimming at a constant speed of 15–18 cm $s^{-1}$ with small variations (figure 5*a*,*e*). This pattern was generated by an uninterrupted succession of type I and/or type II stroke patterns and the maximum speed rarely exceeded 23 cm $s^{-1}$. The second speed pattern showed very large amplitude variations, with regular increases and decreases in speed and a uniform speed frequency distribution (figure 5*b*,*f*). In this case, beetles reached speeds of up to 70 cm $s^{-1}$. Each large speed peak was due to one or two type III stroke patterns (see figure 2 for an example) separated by long periods with no strokes. This resulted in large deceleration phases. The third kind of pattern was a combination of the other two patterns, with speeds of 15–18 cm $s^{-1}$ alternating with periods of much faster speeds (figure 5*c*). Consequently, the speed frequency distribution was bimodal (figure 5*g*). The number of large speed peaks was variable. The final speed pattern was observed following a visual stimulus that scared the beetles. The resulting speed was higher (more than 30 cm $s^{-1}$) and irregular (figure 5*d*), with a mode around 55 cm $s^{-1}$ (figure 5*h*). It resulted from a succession of type III stroke patterns, which were more numerous and closer together than in the second speed pattern.

Finally, we observed a characteristic behaviour of whirligig beetles placed in the plastic tank. Mostly, just after being placed on the water surface, the beetles started swimming in circles a few centimetres in diameter (figure 5*k*, beginning of the trajectory). After several circles, the beetles began to follow an irregular trajectory. A similar behaviour was observed when the beetles rose to the surface after diving. In this case, the beetles began swimming in circles under the water. During this circling behaviour, whirligig beetles produced the first type of speed pattern (figure 5*a*).

### 3.3. Capillarity waves

Characteristic capillarity waves were observed on the water surface for all types of leg kinematics (figure 6). Types I and II produced circular waves of small amplitude, induced by the leg strokes rather than by the front of the body. Each stroke of the leg generated a semicircular wave, and the waves formed by two legs on opposite sides of the body subsequently formed a circle. As whirligig beetles used only their middle legs in type I leg kinematics, each stroke pattern produced a single train of circular waves. Before they joined up, the waves produced by the middle legs had a characteristic bean shape (figure 6*a*, blue).

The type II stroke pattern was generated by a hind stroke followed by a middle leg stroke. It therefore produced two successive trains of circular waves (figure 6*a*). The two waves produced by the hind legs joined up to form a heart-shaped wave before forming a circular wave (figure 6*b*). The waves generated by the middle legs were of the same shape as for type I movements. The wave patterns produced by whirligig beetles using leg kinematics types I and II were similar for beetles starting from a complete stop and for beetles that were already moving. This may have affected wave amplitude, but this parameter was not measured.

Beetles also generated circular waves with the type III stroke pattern, albeit with a greater amplitude. The hind legs produced two semicircular waves behind the body and semicircular waves were also produced in front of the body (figure 6*c*). The waves produced by the middle legs had a smaller amplitude and were, therefore, not always visible. Circular waves were observed only when beetles produced one or two propulsion episodes separated by long periods of deceleration. Beetles moving at high speed (i.e. at least 40 cm $s^{-1}$) for longer periods and using type III leg kinematics generated V-shaped waves in front of their bodies (figure 6*d*), but the waves generated behind the insect by its leg strokes remained semicircular.

The last kind of wave produced by whirligig beetles was of a 'spiral' shape closely resembling the Archimedean spiral (i.e. with constant distance between successive turns), as modelled and observed by Chepelianskii *et al.* (2008; figure 6*e*). Beetles induced this kind of wave in front of their bodies when

Table 1. Mean values of measured parameters ± s.d. for the three types of leg kinematics observed in *G. substriatus* swimming on the water surface (see the text for an explanation of the parameters).

| type of leg kinematics | frequency of propulsion episodes (Hz) | time between hind and middle leg strokes (ms) | maximum hind leg angle (°) | maximum middle leg angle (°) | acceleration (g) | beetle speed (cm s$^{-1}$) |
|---|---|---|---|---|---|---|
| type I | 12.4 (±1.8) | – | – | 103.7(±3.5) | 0.689 (±0.154) | 15.05 (±1.61) |
| type II | 10.6 (±1.8) | 8.9 (±1.3) | 77.1 (±5.6) | 96.8 (±4.8) | 0.801 (±0.219) | 18.34 (±2.13) |
| type III | 36.2 (±8.5) | 10.0 (±1.3) | 105.3 (±8.9) | 79.3 (±7.7) | 2.857 (±0.780) | 48.41 (±6.84) |

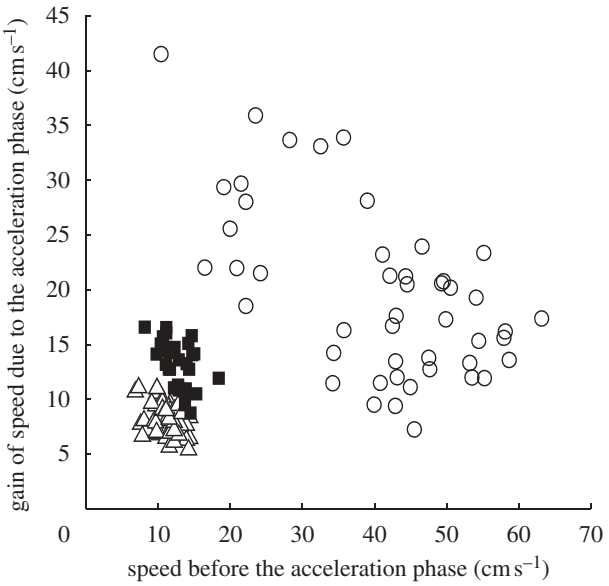


Figure 4. Differentiation of the three types of leg kinematics of *G. substriatus* for all the propulsion episodes analysed, with white triangles for type I, black squares for type II and white circles for type III.

swimming in circles of constant radius, particularly during the circling behaviour described above. Spiral waves were generated by type II and III leg kinematics. The formation of the spiral resulted from deformation of the V-shaped wave. Only one side of the V was produced and it took on a spiral shape due to the propagation of the wave while the insect was still turning and producing the wave. The distance between consecutive turns of the spiral seemed to be greater with type II than with type III leg kinematics (12–13 cm versus 7–8 cm), but too few measurements were taken for statistical analysis.

## 4. DISCUSSION

### *4.1. Types of leg kinematics and propulsion forces*

The whirligig beetle *G. substriatus* uses three different types of leg kinematics when swimming on the water surface: two for swimming at low speed (types I and II) and one for swimming at high speed (type III). Bott (1928) indicated that *G. substriatus* uses only its middle legs when swimming slowly, with a frequency of 4 strokes s$^{-1}$. This pattern could correspond to type I, but we measured a higher stroke frequency for this type of leg kinematics (12.4 strokes s$^{-1}$). The leg kinematics observed by Bott may correspond to irregular stroke patterns, which were excluded in our analysis. Only the high-speed leg kinematics reported here has been described before by Nachtigall (1961, 1974).

The types of leg kinematics differed in terms of their stroke patterns and the maximum angle formed by the legs during these strokes. The maximum angle of the legs, reflecting the extent to which the legs were deformed by resistance forces, can be used to determine the relative importance of the propulsion forces acting on the legs during the power phase of the strokes. Higher maximum angles are associated with stronger forces. Our results for maximal angles show that the propulsion forces provided by the middle legs decrease with increasing beetle speed, whereas the propulsion forces provided by the hind legs increase. The preferential use of the hind legs for high-speed swimming appears logical, as the surface area of the hind legs of *G. substriatus* deployed and their maximum stroke frequency are twice those of the middle legs (Nachtigall 1961). Our results are also consistent with the findings of Larsen (1966), who indicated that amputation of the middle legs did not markedly affect high-speed swimming. It remains unclear why beetles do not make maximum use of both middle and hind legs. It is possible that the middle legs are used primarily to stabilize the trajectory of the beetle, as suggested by Hughes (1958) for diving beetles (*Dysticus*). Stabilization is particularly important in whirligig beetles, the underside of which is smooth and ridge-free. Nachtigall (1974) found that constant and rapid correction was required in *Gyrinus*, due to its instability. Presumably, these beetles are particularly unstable at higher speeds.

The maximum speed measured here was 80 cm s$^{-1}$, which seems to be intermediate between previously reported values. For the genus *Gyrinus*, maximum speeds of 50 cm s$^{-1}$ (Bendele 1986) and 100 cm s$^{-1}$ (Nachtigall 1974) have been reported, whereas maximum speeds of 50 cm s$^{-1}$ (Tucker 1969; Fish & Nicastro 2003) and 144 cm s$^{-1}$ (Vulinec 1987) have been reported for *Dineutus*. This last value appears to be very high and may have been overestimated.

### *4.2. Significance of the speed patterns*

Speed pattern analysis showed that the maximum speed of *G. substriatus* rarely exceeded 23 cm s$^{-1}$ when

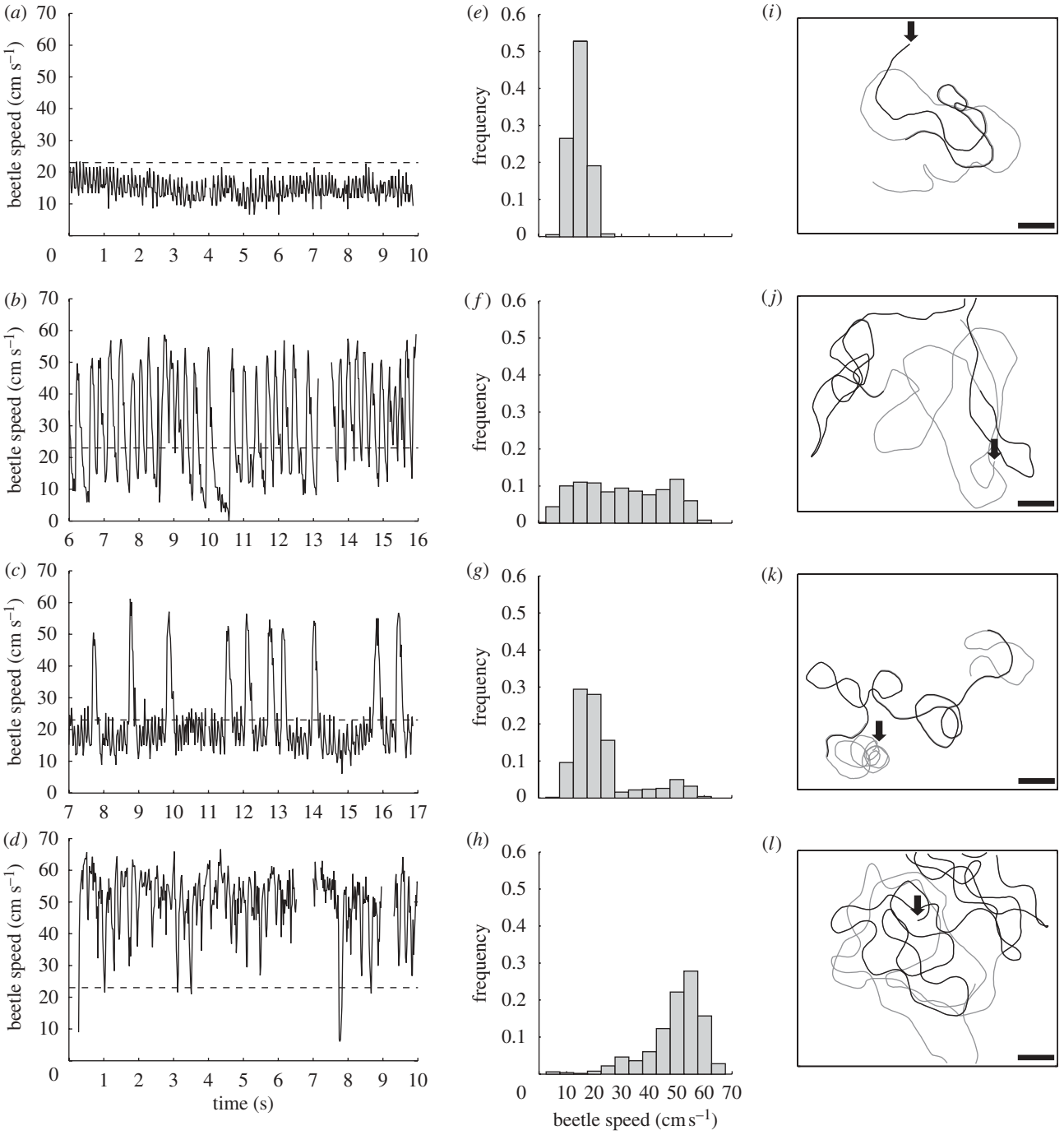


Figure 5. Example of speeds and trajectories for the four main speed patterns observed for *G. substriatus* swimming on the water surface. Panels (*a–d*) show whole-beetle speed over time. The mean speeds of the sequences displayed in (*a–d*) are 14.74, 30.38, 22.80 and 49.75 cm $s^{-1}$, respectively. The dashed line indicates a speed of 23 cm $s^{-1}$, which is the minimum speed required for the generation of surface waves by the beetle's body. Panels (*e–h*) show the speed frequency histograms corresponding to the previous graphs. Panels (*i–l*) show the trajectories of the beetle, in black for the 10 s shown in the previous graphs, and in grey for the others 10 s analysed. The start of the trajectory is indicated by the black arrow and the scale bar represents 10 cm.

swimming with low-speed leg kinematics. This speed corresponds to the minimum speed of waves propagating on the water surface in laboratory conditions, and also to the minimum speed at which a steadily moving object needs to move to produce waves (Lighthill 1978). Consequently, a beetle swimming at speeds lower than 23 cm $s^{-1}$ will not create waves with its body, at least if it moves in an almost straight line at constant speed. Acceleration is inherent to a circling motion, so beetles turning in circles are not limited by a velocity threshold for surface wave production (Chepelianskii *et al.* 2008), as observed in our experiments. Leg strokes always produce waves, presumably due to the unsteady movement of the legs. We hypothesize that beetles do not exceed this speed to avoid generating wave resistance. In this way, the energy invested in the strokes propelling the body forward is not lost in wave drag. This speed corresponds to

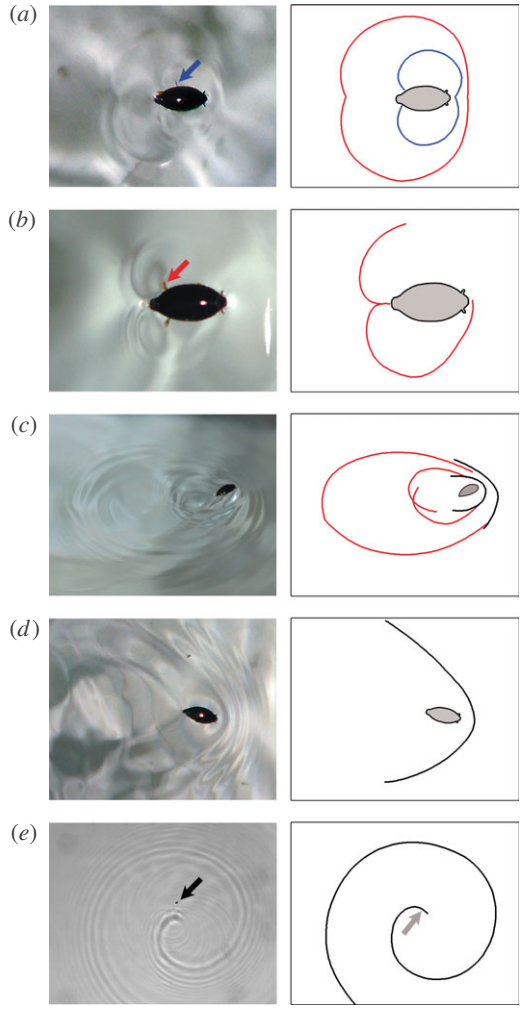


Figure 6. Capillarity waves produced by the different types of leg kinematics of *G. substriatus* swimming on the water surface. The diagrams on the right correspond to the photographs on the left and represent the beetle (in grey) and the shape of the waves produced and visible in the photos. The waves produced by the hind leg strokes are shown in red, the waves produced by the middle leg strokes in blue and the waves produced by the beetle body in black. The blue arrow shows a middle leg, the red arrow indicates a hind leg and the black arrow shows the whole beetle. Waves produced by type I leg kinematics correspond to the blue wave shape induced by the middle leg stroke in (*a*). The waves shown in (*a*) and (*b*) are small circular waves produced by type II leg kinematics. Panels (*c*) and (*d*) show characteristic waves for type III leg kinematics, with a succession of two trains of circular waves (*c*) and V-shape waves (*d*). The spiral wave produced by type II leg kinematics is shown in (*e*). Only the shadows of the waves are visible on the photograph. The light was not directly above the beetle, giving the impression that the insect is not in the centre of the spiral. The grey arrow indicates the real position of the beetle relative to the waves and its direction.

the behaviour generally observed in the field and in laboratory conditions, for undisturbed beetles in groups (Brown & Hatch 1929; Heinrich & Vogt 1980; J. Voise & J. Casas 2008, personal observations).

However, whirligig beetles need to move faster, particularly when trying to escape predators or to cover large distances. In these cases, they use high-speed leg kinematics. The approach of a visual stimulus mimicking a predator creates a fright reaction (Brown & Hatch 1929; Newhouse & Aiken 1986). Beetles then move very fast and try to keep their speed as high as possible. In such situations, beetles produce large numbers of strokes and waste lots of energy, but this high cost is acceptable because the insect's survival is at stake.

The speed pattern characterized by a succession of large-amplitude peaks is typical of intermittent locomotion. The animal displays intermittent locomotion when the forces exerted for movement are applied discontinuously and the pauses are longer than the normal deceleration phase of a propulsion episode (Kramer & McLaughlin 2001). There are several advantages to this type of locomotion, including greater endurance and better environment detection (e.g. Weinstein & Full 1992; Trouilloud *et al.* 2004). This speed pattern was produced by whirligig beetles moving on the water through a succession of bursts of speed. This situation is observed in the field when beetles swim in a straight line while searching for food or favourable conditions (Heinrich & Vogt 1980; personal observations).

### *4.3. Dealing with the resistance forces*

The surface waves produced by the legs may be involved in beetle propulsion, as shown for water striders, which use both vortices and waves produced by the resistance forces acting on the legs for propulsion (Hu *et al.* 2003; Buhler 2007). However, the combination of these resistance forces is problematic when these forces act on the beetle's body to oppose its motion.

Figure 7 shows wave and fluid resistances plotted against beetle speed and the mean speed ($\pm$s.d.) generated by each type of leg kinematics. Fluid resistance increased quadratically with speed. The wave drag is null at speeds below 23 cm $s^{-1}$. However, as soon as beetles reach this speed, they come up against the maximum wave drag, which decreases with increasing speed. The wave resistance curve is characterized by the discontinuity and by the maximal value at the discontinuity. The discontinuity occurs because of the dispersive nature of surface waves. Below the critical speed (i.e. the minimal speed for surface wave production), no wake is produced and wave drag is null. The discontinuous transition predicted by Raphaël & de Gennes (1996) has been discussed in light of the conflicting experimental results obtained (Browaeys *et al.* 2001; Burghelea & Steinberg 2001). Chevy & Raphaël (2003) subsequently showed that the discontinuity of the wave drag depends critically on the experimental conditions, including the position of the water line on the moving in particular. If the object moves at a constant depth, the discontinuity disappears and gives way to a smooth transition. This is not included in the model used here.

The speed at which wave resistance starts to decrease is a function of the size of the object. At a speed of 23 cm $s^{-1}$, a wake is generated and the wavelengths are comparable to the size of the beetle (6 mm). The size of the beetle is thus important, and the wave resistance therefore decreases from 23 cm $s^{-1}$. In other words,

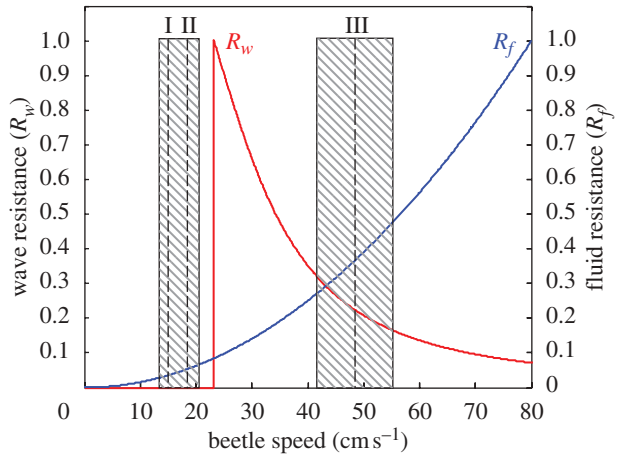


Figure 7. Changes in wave resistance (in red) and fluid resistance (in blue) as a function of the speed of whirligig beetles (*G. substriatus*). Wave resistance is non-dimensioned by its maximum, and fluid resistance is non-dimensioned by its value at 80 cm s$^{-1}$ (0.215 mN), which is the maximum speed observed in our experiments. Dashed lines represent the mean speed for the three types of leg kinematics and shaded rectangles represent the standard errors of these means. Type I (I) and type II (II) have been grouped together, because their standard deviations overlap. These two types of kinematics correspond to low-speed leg kinematics, whereas type III (III) corresponds to high-speed leg kinematics.

there is no speed regime at which the size of the beetle can be neglected.

The relative values obtained for fluid and wave resistances show how these resistances vary as a function of the beetle speed. However, quantitative estimation of both these resistances would be interesting, as it would make it possible to estimate the total resistance. Fluid resistance can be approximated by roughly estimating $c_w$ and $F$ in equation (2.1), assuming that they do not vary with beetle speed. We took a value of 0.3 for $c_w$, which is intermediate between the values obtained for diving beetles *Dysticus* ($c_w = 0.34$) and *Acilius* ($c_w = 0.23$; Nachtigall 1974). We estimated $F$ by measuring the frontal area of the part of the body in contact with the water on 10 beetles (mean: $2.24 \pm 0.46$ mm$^2$). We determined this area as a semi-elliptic area, given by $\pi l(L/2)/2$, with $l$ the maximum height of the lower part of the body (i.e. the maximum height of the body under the water) and $L$ the body width, both as seen from the front. We obtained a value of 0.054 mN for a speed of 40 cm s$^{-1}$, and of 0.215 mN at 80 cm s$^{-1}$, the maximum beetle speed measured in our experiments.

It is much more difficult to estimate the magnitude of the wave resistance. Many studies have investigated the wave drag generated by large objects, such as boats, taking into account gravity waves only (Havelock 1910; Kostyukov 1968; Kelvin 1887). Wave resistance has more recently been investigated for small objects, taking into account both capillary and gravity waves under the restrictive assumption that the object concerned does not touch the water (Raphaël & de Gennes 1996). In this previously described model, Raphaël and de Gennes considered pressure sources much smaller than the capillary length (3 mm for the air–water interface; see notes 8 and 13 in Raphaël & de Gennes 1996). By contrast, if the object is larger than the capillary length, as is the case for this beetle species, an approach in which every point along the object becomes a source in itself might be needed, with the additional problems of wave interference. All current models assume an absence of contact between the object and the water surface. The inclusion of a partially immerged object in the calculation of wave resistance thus remains an unresolved problem.

Nonetheless, we tried to obtain an order of magnitude for the wave resistance as follows. Let us assume that the beetle has no size but does have a weight, which we measured by taking the mean of 10 individuals ($0.147 \pm 0.02828$ mN). According to Raphaël & de Gennes (1996), the order of magnitude of the wave resistance is then given by:

$$R_w = \frac{p^2}{\gamma\kappa^{-1}}, \tag{4.1}$$

with $p$ the pressure force exerted by the object, $\gamma$ the surface tension and $\kappa^{-1}$ the capillary length. The weight of the beetle was considered to correspond to the pressure force. We obtained a value for the wave resistance of 0.100 mN.

These estimates indicate that fluid and wave resistances are of the same order of magnitude. An important consequence of this is that the total resistance has a potential local maximum at the velocity for which wave resistance is maximal. For both fluid and wave resistances, we can delimit two ranges of speed at which the values obtained are at least 50 per cent lower than the maximum. These two ranges should correspond to speed regimes minimizing total resistance. The first range, corresponding to speeds below 23 cm s$^{-1}$, includes the mean speeds generated by low-speed leg kinematics. The other range, corresponding to speeds between 35 and 60 cm s$^{-1}$, includes the mean speed for high-speed leg kinematics (figure 7). The gap between low and high speeds can be accounted for by whirligig beetles avoiding maximal wave drag. These beetles significantly increase their speed to reach the upper value when swimming at the lower value, creating the large peaks observed in the speed patterns. Their maximal speed is also determined by fluid resistance. Thus, whirligig beetles swim in different ways to maintain their speed when resistance forces are weak.

We would like to thank five anonymous reviewers for their valuable comments on the first version of this paper, together with Elie Raphaël and Alexei Chepelianskii for discussions. This work is part of the PhD thesis of J.V. financed by the Région Center under the supervision of J.C.

## REFERENCES

Bendele, H. 1986 Mechanosensory cues control chasing behavior of whirligig beetles (Coleoptera, Gyrinidae). *J. Comp. Physiol. A* **158**, 405–411. (doi:10.1007/BF00603624)

Bott, R. H. 1928 Beitrage zur kenntnis von *Gyrinus natator substriatus* Steph. *Z. Morphol. Oekol. Tiere* **10**, 207–306. (doi:10.1007/BF00410268)

Browaeys, J., Bacri, J. C., Perzynski, R. & Shliomis, M. I. 2001 Capillary-gravity wave resistance in ordinary and magnetic fluids. *Europhys. Lett.* **53**, 209–215. (doi:10.1209/epl/i2001-00138-7)

Brown, C. R. & Hatch, M. H. 1929 Orientation and 'fright' reactions of whirligig beetles (gyrinidae). *J. Comp. Psychol.* **9**, 159–189. (doi:10.1037/h0075551)

Buhler, O. 2007 Impulsive fluid forcing and water strider locomotion. *J. Fluid. Mech.* **573**, 211–236. (doi:10.1017/s002211200600379x)

Burghelea, T. & Steinberg, V. 2001 Onset of wave drag due to generation of capillary-gravity waves by a moving object as a critical phenomenon. *Phys. Rev. Lett.* **86**, 2557–2560. (doi:10.1103/PhysRevLett.86.2557)

Bush, J. W. M. & Hu, D. L. 2006 Walking on water: biolocomotion at the interface. *Annu. Rev. Fluid Mech.* **38**, 339–369. (doi:10.1146/annurev.fluid.38.050304.092157)

Bush, J. W. M., Hu, D. L. & Prakash, M. 2008 The integument of water-walking arthropods: form and function. In *Advances in insect physiology: insect mechanics and control*, vol. 34 (eds J. Casas & S. J. Simpson), pp. 117–192. London, UK: Elsevier Academic Press.

Chepelianskii, A. D., Chevy, F. & Raphaël, E. 2008 Capillary-gravity waves generated by a slow moving object. *Phys. Rev. Lett.* **100**, 074504. (doi:10.1103/PhysRevLett.100.074504)

Chevy, F. & Raphaël, E. 2003 Capillary gravity waves: a 'fixed-depth' analysis. *Europhys. Lett.* **61**, 796–802. (doi:10.1209/epl/i2003-00304-5)

Dean, R. G. & Dalrymple, R. A. 1991 *Water wave mechanics for engineers and scientists*. Advanced Series on Ocean Engineering. Singapore: World Scientific.

Eggers, F. 1926 Die mutmaBliche Funktion des Johnstonschen sinnesorgans bei. *Gyrinus. Zool. Anz.* **68**, 184–192.

Eggers, F. 1927 Nähere Mitteilungen über das Jonhstonsche Sinnesorgan und über das Ausweichvermögen der Taumelkäfer. *Zool. Anz.* **71**, 136–156.

Fish, F. E. & Nicastro, A. J. 2003 Aquatic turning performance by the whirligig beetle: constraints on maneuverability by a rigid biological system. *J. Exp. Biol.* **206**, 1649–1656. (doi:10.1242/jeb.00305)

Hatch, M. H. 1927 The morphology of Gyrinidae. *Pap. Mich. Acad. Sci. Arts Lett.* **7**, 311–350.

Havelock, T. H. 1910 The wave-making resistance of ships: a study of certain series of model experiments. *Proc. R. Soc. Lond. A* **84**, 197–208.

Heinrich, B. & Vogt, F. D. 1980 Aggregation and foraging behavior of whirligig beetles (Gyrinidae). *Behav. Ecol. Sociobiol.* **7**, 179–186. (doi:10.1007/BF00299362)

Hu, D. L., Chan, B. & Bush, J. W. M. 2003 The hydrodynamics of water strider locomotion. *Nature* **424**, 663–666. (doi:10.1038/nature01793)

Hughes, G. M. 1958 The co-ordination of insect movements. *J. Exp. Biol.* **35**, 367–583.

Kelvin, L. 1887 On the waves produced by a single impulse in water of any depth, or in a dispersive medium. *Proc. R. Soc. Lond.* **42**, 80–83. (doi:10.1098/rspl.1887.0017)

Kolmes, S. A. 1983 Ecological and sensory aspects of prey capture by the whirligig beetle *Dineutus discolor* (Coleoptera, Gyrinidae). *J. N. Y. Entomol. Soc.* **91**, 405–412.

Kolmes, S. A. 1985 Surface vibrational cues in the precopulatory behavior of whirligig beetles. *J. N. Y. Entomol. Soc.* **93**, 1137–1140.

Kostyukov, A. A. 1968 *Theory of ship waves and wave resistance*. Iowa, IA: Effective Commun. Inc.

Kramer, D. L. & McLaughlin, R. L. 2001 The behavioral ecology of intermittent locomotion. *Am. Zool.* **41**, 137–153. (doi:10.1093/icb/41.2.137)

Larsen, O. 1966 On the morphology and function of the locomotor organs of the Gyrinidae and other Coleoptera. *Opuscula Entomol. Supplement.* **30**, 1–241.

Lee, S. Y., Bush, J. W. M., Hosoi, A. E. & Lauga, E. 2008 Crawling beneath the free surface: water snail locomotion. *Phys. Fluids* **20**, 082106. (doi:10.1063/1.2960720)

Lighthill, J. 1978 *Waves in fluids*. New York, NY: Cambridge University Press.

Nachtigall, W. 1961 Funktionelle morphologie, kinematik und hydromechanik des ruderapparates von. *Gyrinus. Z. vergl. Physiol.* **45**, 193–226. (doi:10.1007/BF00297764)

Nachtigall, W. 1974 Locomotion: mechanics and hydrodynamics of swimming in aquatic insects. In *The physiology of Insecta*, vol. III (ed. M. Rockstein), pp. 381–432. New York, NY: Academic Press.

Nachtigall, W. 1981 Hydromechanics and biology. *Biophys. Struct. Mech.* **8**, 1–22. (doi:10.1007/BF01047102)

Newhouse, N. J. & Aiken, R. B. 1986 Protean behaviour of a neustonic insect: factors releasing the fright reaction of whirligig beetles (Coleoptera: Gyrinidae). *Can. J. Zool.* **64**, 722–726. (doi:10.1139/z86-106)

Raphaël, E. & de Gennes, P. G. 1996 Capillary gravity waves caused by a moving disturbance: wave resistance. *Phys. Rev. E* **53**, 3448–3455. (doi:10.1103/PhysRevE.53.3448)

Reinig, H.-J. & Uhlemann, H. 1973 Über das Ortungsvermögen des Taumelkäfers *Gyrinus substriatus* Steph. (Colepotera, Gyrinidae). *J. Comp. Physiol.* **84**, 281–298. (doi:10.1007/BF00694227)

Rudolph, P. 1967 Zum Ortungsverfahren von *Gyrinus substriatus* Steph. *Z. vergl. Physiol.* **56**, 341–375. (doi:10.1007/BF00298054)

Suter, R. B., Rosenberg, O., Loeb, S., Wildman, H. & Long, J. H. 1997 Locomotion on the water surface: propulsive mechanisms of the spider *Dolomedes triton*. *J. Exp. Biol.* **200**, 2523–2538.

Trouilloud, W., Delisle, A. & Kramer, D. L. 2004 Head raising during foraging and pausing during intermittent locomotion as components of antipredator vigilance in chipmunks. *Anim. Behav.* **67**, 789–797. (doi:10.1016/j.anbehav.2003.04.013)

Tucker, V. A. 1969 Wave-making by whirligig beetles (Gyrinidae). *Science* **166**, 897–899. (doi:10.1126/science.166.3907.897)

Vulinec, K. 1987 Swimming in whirligig beetles (Coleoptera: Gyrinidae): a possible role of the pygidial gland secretion. *Coleopt. Bull.* **41**, 151–153.

Weinstein, R. B. & Full, R. J. 1992 Intermittent exercise alters endurance in an eight-legged ectotherm. *Am. J. Physiol. Regul. Integr. Comp. Physiol.* **262**, R852–R859.

Wilde, J. d 1941 Contribution to the physiology of the Johnston organ and its part in the behavior of the. *Gyrinus. Arch. Neer. de Physiol.* **25**, 381–400.

Winkelman, D. L. & Vinyard, G. L. 1991 Gyrinid searching tactics: empirical observations and a tactical model. *Behav. Ecol. Sociobiol.* **28**, 345–351. (doi:10.1007/BF00164384)

Ziegler, F. 1998 *Mechanics of solids and fluids*. New York, NY: Springer-Verlag.